ResearchGate

See discussions, stats, and author profiles for this publication at: https://www.researchgate.net/publication/6343537

A Calorimetry and Light Scattering Study of the Formation and Shape Transition of Mixed Micelles of EO 20 PO 68 EO 20 Triblock Copolymer (P123) and Nonionic Surfactant (C 12 EO 6)

ARTICLE *in* THE JOURNAL OF PHYSICAL CHEMISTRY B · JUNE 2007

Impact Factor: 3.3 · DOI: 10.1021/jp071101n · Source: PubMed

CITATIONS
53

READS
45

5 AUTHORS, INCLUDING:

Karin Schillén
Lund University
80 PUBLICATIONS **2,867** CITATIONS
SEE PROFILE

Watson Loh
University of Campinas
105 PUBLICATIONS **2,238** CITATIONS
SEE PROFILE

Available from: Karin Schillén
Retrieved on: 26 January 2016

A Calorimetry and Light Scattering Study of the Formation and Shape Transition of Mixed Micelles of $EO_{20}PO_{68}EO_{20}$ Triblock Copolymer (P123) and Nonionic Surfactant ($C_{12}EO_6$)

David Löf,[†] Anna Niemiec,[‡] Karin Schillén,*[,†] Watson Loh,*[,‡] and Gerd Olofsson[†]

Physical Chemistry 1, Chemical Center, Lund University, P. O. Box 124, SE-221 00 Lund, Sweden, and Instituto de Quimica, Universidade Estadual de Campinas, C.P. 6154, 13084-970, Campinas, SP, Brazil

Received: February 8, 2007

The interaction between the nonionic surfactant $C_{12}EO_6$ and the poly(ethylene oxide)−poly(propylene oxide)−poly(ethylene oxide) triblock copolymer $EO_{20}PO_{68}EO_{20}$ (P123) has been investigated by means of isothermal titration and differential scanning calorimetry (DSC) as well as static and dynamic light scattering (SLS and DLS). P123 self-assembles in water into spherical micelles at ambient temperatures. At raised temperatures, the DSC data revealed a sphere-to-rod transition of the P123 micelles around 60 °C. $C_{12}EO_6$ interacts strongly with P123 micelles in aqueous solution to give mixed micelles with a critical micelle concentration (cmc) well below the cmc for pure $C_{12}EO_6$. The presence of $C_{12}EO_6$ also lowers the critical micelle temperature of P123 so aggregation starts at significantly lower temperatures. A new phenomenon was observed in the P123−$C_{12}EO_6$ system, namely, a well-defined sphere-to-rod transition of the mixed micelles. A visual phase study of mixtures containing 1.00 wt % P123 showed that in a narrow concentration range of $C_{12}EO_6$ both the sphere-to-rod transition and the liquid−liquid phase separation temperature are strongly depressed compared to the pure P123−water system. The hydrodynamic radius of spherical mixed micelles at a $C_{12}EO_6$/P123 molar ratio of 2.2 was estimated from DLS to be 9.1 nm, whereas it is 24.1 nm for the rodlike micelles. Furthermore, the hydrodynamic length of the rods at a molar ratio of 2.2 is in the range of 100 nm. The retarded kinetics of the shape transition was detected in titration calorimetric experiments at 40 °C and further studied by using time-resolved DLS and SLS. The rate of growth, which was slow (>2000 s), was found to increase with the total concentration.

Introduction

The triblock copolymers composed of poly(ethylene oxide) (PEO) and poly(propylene oxide) (PPO) are nonionic, water-soluble, low-molar-mass polymers often abbreviated as PEO−PPO−PEO or $EO_nPO_mEO_n$.[1] These copolymers are produced in a broad range of compositions,[2] and they are widely used in industrial and scientific applications.[3−6] In dilute aqueous solutions, the PEO−PPO−PEO copolymers may self-assemble to form micelles, with a hydrophobic core containing PPO, which is protected from the surrounding water by a water-swollen PEO corona as established by light, X-ray (SAXS), and neutron (SANS) scattering investigations.[7−11] The thermodynamic characteristics of micelle formation derived from differential scanning calorimetry (DSC) and steady-state fluorescence spectrocopy experiments have been reported.[12,13] Three excellent reviews of the physical chemistry of PEO−PPO−PEO copolymers in water can be found in refs 14−16. In PEO−PPO−PEO−water systems, the micelles are spherical at ambient temperatures but may change in shape at elevated temperatures, presenting a sphere-to-rod transition.[10,17−20] The change in shape is a combination of the conformational changes of PEO and a release of the imposed stretching of PPO blocks in the micellar core which is accompanied by the decrease of the cross-sectional radius of the micelles.[10,17,21] Salts like NaCl and KF lower the solubility of PEO in water and thus lower both the temperature for micelle formation and sphere-to-rod transition as well as the phase separation temperature.[22−24]

The formation of micelles of PEO−PPO−PEO copolymers is also promoted by hydrophobic substances, such as alcohols (pentanol or higher alcohols), benzene, and tributylphosphate.[25−30] The authors of ref 28 concluded that the solubilization plays a role similar to that of a temperature increase, that is, an increase of the hydrophobic character of the core and reduced hydration of the shell. Both effects promote the formation of micelles.

The interaction between PEO−PPO−PEO copolymers and nonionic C_iEO_j surfactants and how that affects the copolymer self-assembly has been less investigated. The $C_{12}EO_6$ surfactant interacts synergistically with the copolymers F127 ($EO_{97}PO_{69}EO_{97}$) and L64 ($EO_{13}PO_{30}EO_{13}$) to form mixed micelles, as shown in two recent studies.[31,32] A study of the ternary phase diagram of the copolymer P105 ($EO_{37}PO_{58}EO_{37}$) with $C_{12}EO_5$ in water showed that these two amphiphiles although of different sizes are miscible over large ranges of composition and temperature.[33]

We have performed in a separate study a static and dynamic light scattering (SLS and DLS) investigation of the self-assembly of the copolymer P123 ($EO_{20}PO_{68}EO_{20}$) and $C_{12}EO_6$ in dilute aqueous solution.[34] The physical properties of the P123−$C_{12}EO_6$ mixed micelles such as molar mass and hydrodynamic radius were determined for varying amounts of $C_{12}EO_6$ and at temperatures varying from 25 to 43 °C.[34] The measurements showed that, at constant temperature, the size of the spherical mixed micelles decreases with increasing $C_{12}EO_6$ content up to a certain threshold, above which wormlike micelles form,

* Corresponding authors. E-mail: Karin.Schillen@fkem1.lu.se (K.S.); wloh@iqm.unicamp.br (W.L.).
[†] Lund University.
[‡] Universidade Estadual de Campinas.

10.1021/jp071101n CCC: $37.00 © 2007 American Chemical Society
Published on Web 05/09/2007

similar to pure $C_{12}EO_6$ micelles; see, for example, refs 35 and 36 and references therein.

The purpose of this study was to further investigate the interparticle interaction and the mixed micellization process in the P123−$C_{12}EO_6$ system by using differential scanning and isothermal titration calorimetry (ITC), SLS, and DLS. We have observed a shape transition of the P123−$C_{12}EO_6$ mixed micelles from spherical to rodlike. The retarded kinetics of this transition was studied by means of time-resolved SLS and DLS. It was also detected in titration calorimetric experiments. Such a shape transition has to our knowledge not been reported earlier. The sphere-to-rod transition temperature varied with the composition of the system and showed a minimum of about 40 °C for a $C_{12}EO_6$/P123 molar ratio between 2 and 3. At the same composition, the liquid−liquid phase separation temperature showed a pronounced minimum.

Experimental Section

Materials. The PEO−PPO−PEO triblock copolymer (denoted P123) has an average composition of $EO_{20}PO_{68}EO_{20}$ and a nominal molar mass of 5750 g mol^{-1}. The sample was a kind gift from BASF Corporation, Performance Chemicals, Mount Olive, NJ, and used without further treatment. P123 is polydisperse both in molar mass and in composition, which was previously found using gel permeation chromatography (GPC).[37] Hexa(ethylene glycol) monododecyl ether ($C_{12}EO_6$) was obtained from Nikko Chemicals Co., Tokyo, Japan, and used as received. The molar mass is 450.7 g mol^{-1}. Judging from the gas chromatogram provided by the manufacturer, the purity of the sample was better than 99%. Water purified by a Milli-Q system (Millipore Corporation, Bedford, MA) was used in all solutions. The stock solutions of the P123 and $C_{12}EO_6$ were prepared by weight and left to equilibrate over night in a refrigerator at 4 °C. We estimate the relative uncertainty in the concentrations of solutions used in our study to be about 0.01.

Differential Scanning Calorimetry. Differential scanning calorimetry (DSC) measurements were made using Microcal MC-2 and Microcal VP-DSC high-sensitivity differential scanning calorimeters (Microcal Inc., Northampton, MA) in the temperature range from 5 °C to usually 80 °C. The sample volume was 1.2 mL in the MC-2 instrument and 0.5 mL in the VP-DSC one. The samples were kept at 5 °C for 20 min before the scan was started. The DSC thermograms record the differential power required to maintain the sample and the reference at the same temperature while scanning the temperature at a constant rate. Reference thermograms were recorded under the same conditions by filling both cells with water.

Isothermal Titration Calorimetry. The isothermal titration experiments were performed using a Microcal VP-ITC microcalorimeter. The experiments consisted of consecutive injections of concentrated surfactant solution into the calorimeter cell that initially contained 1.44 mL of dilute P123 solution or water. The samples were added from a gastight syringe, the tip of which is modified to act as a stirrer. Injection volumes varied between 3 and 15 μL. The time between injections was usually 10 min, but it was increased to 30 min in regions with slow equilibration. As the surfactant solution is added, the cell volume is kept constant by an overflow of solution, which is taken into account in the calculations of actual concentrations of polymer and surfactant in the cell. Measurements were made at 15 and 40 °C.

Phase Studies. Samples of varying $C_{12}EO_6$/P123 molar ratios were prepared in closed glass vials that were kept in a thermostatic water bath. The temperature was increased in steps of 2 °C, and the samples were inspected 12 and 24 h after the temperature was changed.

Dynamic and Static Light Scattering. The setup for the dynamic light scattering (DLS) and static light scattering (SLS) measurements employed an ALV/DLS/SLS-5000F, CGF-8F-based compact goniometer system from ALV-GmbH, Langen, Germany, with vertical−vertical polarization geometry using a Glan−Thomson polarizer and a Glan prism. The light source is a Nd:YAG solid-state Compass-DPSS laser (Coherent Inc., Santa Clara, CA), which operates at 532 nm with a fixed output power of 400 mW that can be varied using an attenuator from Newport Inc. The cylindrical light scattering cell is immersed in a refractive-index-matching liquid (*cis*-decahydronaphthalene or decaline) kept in a cylindrical quartz container (VAT). The detection system includes a near-monomodal optical fiber and two matched photomultipliers in a pseudo-cross geometry. Two multiple τ digital correlators with 320 spaced channels were utilized with an initial sampling time of 12.5 ns to construct the time correlation function (TCF) (pseudo-cross or auto) of the scattered intensity, $G^{(2)}(t)$. The static light scattering intensity was monitored and normalized to the incoming laser intensity. The temperature was varied and controlled to within ±0.01 °C. A detailed description of the DLS/SLS equipment can be found in ref 37. Prior to the measurements, the solutions were equilibrated at room temperature for at least 20 min before being filtered directly into the cylindrical light scattering cell (both quartz and borosilicate cells were used) through a sterile, hydrophilic Minisart filter with a 0.2 μm pore diameter (Sartorius, Germany).

DLS Data Analysis. The analysis of the DLS data was directly performed on the normalized experimentally measured time correlation function of the scattering intensity, $g^{(2)}(t)$. The model used in the fitting procedures is expressed with respect to the normalized TCF of the electric field, $g^{(1)}(t)$, which is related to $g^{(2)}(t)$ by Siegert's relation:

$$g^{(2)}(t) - 1 = \beta |g^{(1)}(t)|^2 \tag{1}$$

where t is the lag time and β is the coherence factor (≤ 1) that takes deviations from the ideal correlation and the experimental geometry into account.

For a system that exhibits a multiexponential decay with a distribution of relaxation times, τ, $g^{(1)}(t)$ is described by a Laplace transform:

$$g^{(1)}(t) = \int_{-\infty}^{\infty} \tau A(\tau) \exp(-t/\tau)\, \mathrm{d} \ln \tau \tag{2}$$

where $\tau = \Gamma^{-1}$ and Γ is the relaxation or frequency rate.

The relaxation time distribution, $A(\tau)$, can be obtained by performing an inverse Laplace transformation of the normalized intensity correlation function (with $g^{(1)}(t)$ expressed as in eq 2) using a nonlinear constrained regularization method that minimizes the sum of the squared differences between the experimental and calculated $g^{(2)}(t)$.[38] The REPES algorithm incorporated into the GENDIST analysis package was used.[18] It iterates a penalizing parameter to the probability of rejecting the penalized solution selected by the user. In all analyses, the "probability-to-reject" term was set to 0.5. The relaxation time distributions presented are expressed in equal area representation as $\tau A(\tau)$ vs $\log(\tau/\mathrm{ms})$.[38]

The collective or mutual diffusion coefficient, D, for particles undergoing translational motion, is related to the relaxation rate, Γ, which is obtained in the output of the analysis:

$$D = \lim_{q \to 0}\left(\frac{\Gamma}{q^2}\right) \quad (3)$$

where q is the magnitude of the scattering vector [$q = 4\pi n_0 \sin(\theta/2)/\lambda$, where n_0 is the refractive index of the solvent (here water), λ is the incident wavelength, and θ is the scattering angle]. In this study, D is thus obtained from the slope of $\Gamma = f(q^2)$. The factor $(1 - \phi)^2$, where ϕ is the volume fraction of the aggregate, has been omitted in the calculations of D, since it only becomes important in concentrated solutions.[39]

The apparent or effective hydrodynamic radius at a finite particle concentration can be calculated from D using the Stokes−Einstein relation:

$$R_{H,app} = \frac{kT}{6\pi\eta_0 D} \quad (4)$$

where k denotes Boltzmann's constant, T is the absolute temperature, and η_0 is the viscosity of water.

Results

DSC Measurements. DSC temperature scans were made on P123 solutions containing 1.00 wt % copolymer and varying amounts of $C_{12}EO_6$, from 5 °C up to usually 80 °C at a scan rate of 1 °C min^{-1}. Varying the scan rate between 0.5 and 1.5 °C min^{-1} did not significantly change the recorded C_p curves, even for a solution with a $C_{12}EO_6$/P123 molar ratio (MR) of about 2.2 (see below). The results of the DSC measurements are summarized in Figure 1, which shows typical DSC traces, and in Table 1, which gives characteristic temperature and enthalpy values for the observed transitions. Figure 1a shows DSC traces where apparent C_p is plotted against temperature for samples containing $C_{12}EO_6$/P123 molar ratios up to 2.2. The concentration of P123 was constant at 1.00 wt % equal to 1.76 mmol L^{-1}.

The traces show one large peak characterized by a T_{onset} value, defined as the temperature at the intersection of the extrapolated linear ascent of the peak with the extrapolated baseline and a T_m value, which is the temperature of the peak maximum. The enthalpy of aggregation, ΔH_{agg}, was calculated from the area under the peak and expressed in kilojoules per mole of P123. Values of T_{onset}, T_m, and ΔH_{agg} are given in columns 2−4 in Table 1. The uncertainty in T_{onset} and T_m is about ±1 °C for pure P123 solution, while it is ±2 °C for T_{onset} for mixtures. The large peak in the curve for pure P123 represents the formation of block copolymer micelles with a critical micelle temperature (cmt) equal to T_{onset}. Values of T_m are constant and the same from pure P123 to mixtures with a MR up to 1.1. Also, values of ΔH_{agg} are not significantly changed for these mixtures. However, there is a significant decrease of T_{onset} from 17 to 13 °C at a MR equal to 1.1. This indicates that the presence of small amounts of $C_{12}EO_6$ induces aggregation of P123 and lowers its cmt. The slight shoulders observed in the peaks for MR = 0.7 and 1.1 are worth noticing. Solutions with MR = 2.2 show a significant decrease in T_m to 16 °C, while T_{onset} is unchanged and ΔH_{agg} is significantly affected. The shoulder on the left-hand side of the peak has disappeared. It is possible that the process associated with the shoulder now has become dominant and is characterized by the new T_m value. DSC traces for samples with a MR between 2.2 and 11 are shown in Figure 1b, and their characteristic values are listed in Table 1.

In this composition range, T_m stays constant at about 16 °C while T_{onset} decreases to below 10 °C. There also seems to be a significant decrease in ΔH_{agg}. For samples with a MR equal to 46, the aggregation peak is shifted to lower temperatures and only the top of the transition peak could be recorded.

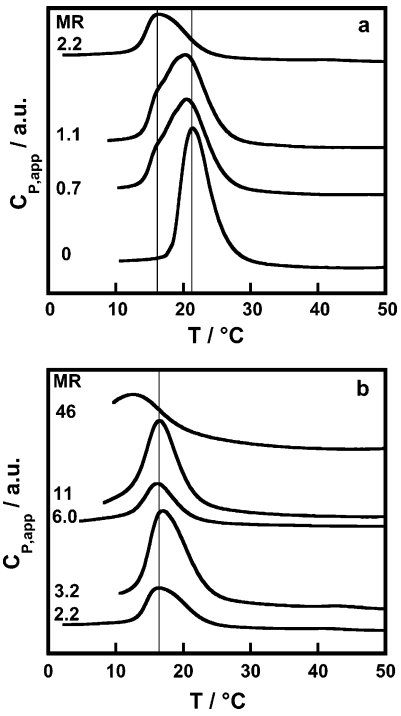

Figure 1. DSC curves showing the main aggregation peak of 1.0 wt % P123 with varying amounts of $C_{12}EO_6$: (a) $C_{12}EO_6$/P123 molar ratios (MR) from 0 to 2.2; (b) MR from 2.2 to 46. The vertical lines at 16 and 21 °C indicate T_m.

TABLE 1: Summary of Data for Transitions Observed in DSC Curves of $C_{12}EO_6$ Mixtures with P123

molar ratio	first peak T_{onset} (°C)	first peak T_m (°C)	first peak ΔH_{agg} (kJ mol^{-1})	second peak T_m(sphere−rod) (°C)	T_{ps} (°C)
0	17	21	460 ± 10	61	79 (>70)[a]
0.07	16	21	440 ± 15	61	77
0.7	14	21	440 ± 15	58	∼75 (>70)
1.1	13	20	430 ± 15	58	∼72
2.2	12	16	440 ± 15	41	56 (>70)
3.2	11	17	380 ± 25	43	57
6	<10	16	390 ± 15	∼52	65 (66)
11	<10	16	360 ± 35	∼54	67 (68)
46	<10	∼12	−	−	54 (54)

[a] Temperature values in parentheses refer to data taken from the visual observations summarized in Figure 3.

At temperatures above the main aggregation peak, the DSC curves show small broad peaks, which we ascribe to a sphere-to-rod transition of the aggregates. At higher temperatures, there are steps in the apparent C_p, which indicate liquid−liquid phase separation. Enlargements of the DSC traces in the temperature region above the main transition peak are shown in Figure 2.

Values for temperatures of the maximum of the second peak, T_m(sphere−rod), and of phase separation, T_{ps}, are shown in columns 5 and 6 of Table 1. Solutions with molar ratios of 2.2 and 3.2 give the narrowest and best-defined peaks with a width of 6−7 °C. At both higher and lower molar ratios, the peaks had a width of about 15 °C. The area of the peaks corresponds to about 10 kJ mol^{-1}, which would represent the enthalpy change for the sphere-to-rod transition. In Figure 2, the values for the transition temperatures for mixtures with different compositions are joined by lines to help comparison with results of the phase studies (see below).

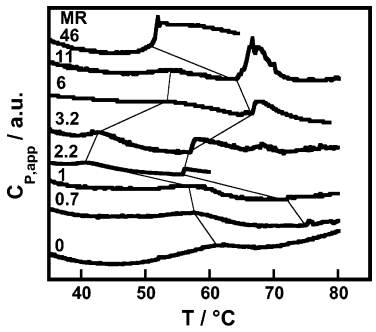

Figure 2. Enlargements of DSC curves above the aggregation peak for 1.0 wt % P123 and $C_{12}EO_6$/P123 molar ratios (MR) from 0 to 46. Values for the transition temperatures (sphere-to-rod and phase separation) are joined by lines as guides for the eye.

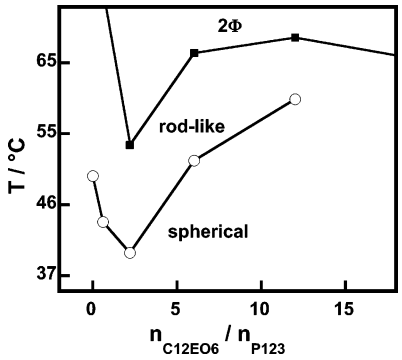

Figure 3. Phase map derived from visual observations (■, ○) of transitions in mixtures of 1.0 wt % P123 with varying amounts of $C_{12}EO_6$ expressed as molar ratio $n_{C_{12}EO_6}/n_{P123}$. The first transition line represents the onset of turbidity, whereas the second transition is at the temperature where macroscopic (liquid−liquid) phase separation was observed.

In DSC traces of pure $C_{12}EO_6$ solution, a small, fairly broad, peak is seen, corresponding to enthalpy changes of about 1−2 kJ mol^{-1}. In 10 mmol L^{-1} solutions, it is centered at 27 °C, and in 50 mmol L^{-1} solutions, at 21 °C. This peak most probably arises from the growth of $C_{12}EO_6$ micelles from spheres to elongated cylinders, as observed by Grell et al. in analogous $C_{14}EO_8$ and $C_{16}EO_8$ systems.[40,41] It has also been observed in 10 mmol L^{-1} $C_{12}EO_6$ solutions,[31] but the authors ascribed the peak to the formation of micelles of $C_{12}EO_6$, which is not correct as the concentration is well above the critical micelle concentration (cmc) of 6.5×10^{-5} mol L^{-1}.[42]

Phase Map. The phase map in Figure 3, based on visual inspection of P123−$C_{12}EO_6$ mixtures as a function of temperature, indicates a transition detected from the appearance of the first signs of turbidity and liquid−liquid phase separation.

The samples started to become turbid at the temperature where the second small peak appears in the DSC curves; see Figure 2 and T_m(sphere−rod) in Table 1. Also, the temperatures for phase separation agree well with temperatures deduced from the DSC curves. The sphere-to-rod transition and liquid−liquid phase separation temperatures move down and then up in the same way in both observations as the molar ratio of the mixture passes the value of 2−3. For the mixture with the highest $C_{12}EO_6$ content, MR = 46, the phase separation temperature correlated well with T_{ps} from the DSC study. The cloud point of a pure $C_{12}EO_6$ solution of the same concentration, 0.08 mol L^{-1}, is about 49 °C,[43] and that of a 1 wt % P123 solution is 90 °C.[2]

ITC Measurements. Figure 4 shows a calorimetric titration curve from consecutive additions of a micellar solution of 1.00 wt % $C_{12}EO_6$ to a 0.30 wt % P123 solution at 15 °C.

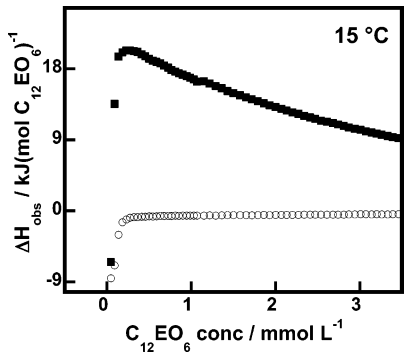

Figure 4. Observed enthalpy changes from the addition of 1.0 wt % $C_{12}EO_6$ to 0.3 wt % P123 solution (■) and to water (○) at 15 °C.

Under these conditions, P123 will be completely in the form of unimers, as shown by DSC measurements; see Figure 1. The curve for dilution of the $C_{12}EO_6$ solution in water is included. At 15 °C, the cmc of $C_{12}EO_6$ is estimated to be 8.3×10^{-5} mol L^{-1} and ΔH_{mic} to be 21.4 kJ mol^{-1} from results reported in ref 42. The first couple of injections in the dilution series give exothermic enthalpy values, showing that the concentration in the calorimeter cell is below the cmc. Further injections increased the concentration to above the cmc, and the enthalpy of dilution of the $C_{12}EO_6$ solution in water became small and close to zero. The first injection into the copolymer solution was exothermic, which indicates that part of the added $C_{12}EO_6$ micelles break up to monomers. Further addition of $C_{12}EO_6$ to P123 solution gave large positive enthalpy changes, which are not expected from the interaction with unimers of P123. Addition of $C_{12}EO_6$ to PPO or PEO solutions does not give measurable enthalpy changes, as observed in previous studies[31] and by us. However, DSC curves show that, already at a $C_{12}EO_6$ concentration of 1 mmol L^{-1}, a significant fraction of P123 is in the form of micelles at 15 °C; see curve for MR = 0.7 in Figure 1. This means that $C_{12}EO_6$ induces aggregation of the polymer to form mixed micellar aggregates. In 0.30 wt % P123, the aggregation starts at about 0.1 mmol L^{-1}. In the same way, addition of $C_{12}EO_6$ to solutions of F127 ($EO_{97}PO_{69}EO_{97}$) and L64 ($EO_{13}PO_{30}EO_{13}$) at temperatures below their cmt in water was found to give large enthalpy increases (endothermic process) from induced aggregation of these copolymers.[31,32]

Addition of $C_{12}EO_6$ (10.0 wt %) to 1.00 wt % P123 solution at 40 °C gave the titration curve shown in Figure 5a. The first injections gave enthalpy values of about 6 kJ mol^{-1} of $C_{12}EO_6$; after that, there was a sudden decrease to a pronounced (exothermic) minimum at a $C_{12}EO_6$/P123 molar ratio of 2.1. After the minimum, the observed enthalpies increased to about 2 kJ mol^{-1}. Further addition of $C_{12}EO_6$ gave a steady decrease in enthalpy changes that became zero and crossed the curve for dilution of $C_{12}EO_6$ in water at around 18 mmol L^{-1} to become slightly exothermic at higher concentrations.

Titration of 0.10 wt % P123 with 1.00 wt % $C_{12}EO_6$, see Figure 5b, showed that $C_{12}EO_6$ started to interact with the aggregated P123 already from the first addition, which gave a concentration of 1.5×10^{-5} mol L^{-1}. Further injections gave about the same endothermic enthalpy changes, corresponding to approximately 3 kJ mol^{-1} of $C_{12}EO_6$. At a molar ratio of 3.1 (±0.1), there was a sudden drop in the observed enthalpy values to about −1 kJ mol^{-1}. After the minimum, the same behavior as that for 1.00 wt % P123 solution was observed; see Figure 5b. The same pattern was observed for titration into 0.30 wt % P123 solutions, except that the minimum enthalpy value observed was about 0.9 kJ mol^{-1} and occurred at a molar ratio of 2.4. The crossing of the surfactant dilution line was at a molar

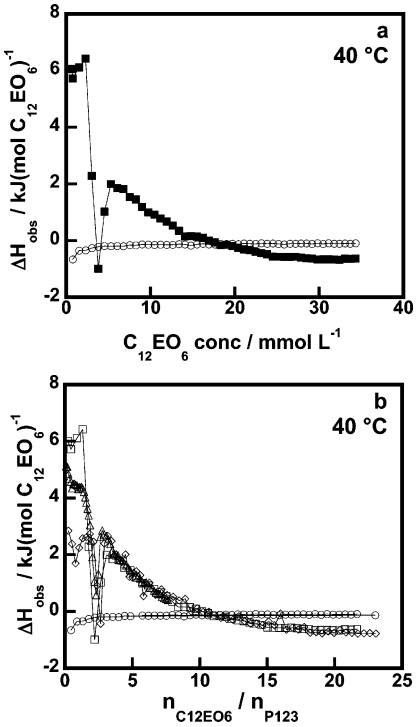

Figure 5. (a) Observed enthalpy changes from the addition of 10 wt % $C_{12}EO_6$ to 1.0 wt % P123 solution (■) at 40 °C. (b) Titration experiments with the addition of $C_{12}EO_6$ to 0.1 (◇), 0.3 (△), and 1 (□) wt % P123 solutions at 40 °C, expressed as a function of $C_{12}EO_6$/P123 molar ratio. Also included in panels a and b are the surfactant addition to water (○).

ratio of about 12, as for the other curves. Measurements with 1.50 wt % P123 (not shown) differed only in the initial values for observed enthalpies, about 6 kJ mol^{-1}, and with the minimum positioned at a molar ratio of 2.1.

Experiments with dilution of 1.00 wt % $C_{12}EO_6$ in water at 40 °C gave observed enthalpy changes consistent with a cmc of 5.3×10^{-5} mol L^{-1} and enthalpy of micelle formation of 5.5 ± 0.5 kJ mol^{-1}.[42,44] Dilution of both 1.00 and 10.0 wt % $C_{12}EO_6$ at concentrations above the cmc gave enthalpy values close to zero.

At 40 °C, P123 copolymer will be mostly in the form of micellar aggregates, since this temperature is well above the cmt of P123 and micelle formation is complete; see DSC curves in Figure 1. The calorimetric titrations show that $C_{12}EO_6$ interacts with P123 already at concentrations as low as 1.5×10^{-5} mol L^{-1}. The constant positive enthalpy values observed until the critical molar ratio region is reached indicate that $C_{12}EO_6$ monomers are solubilized in the P123 micelles, forming mixed aggregates.[34] After this initial solubilization, there is a drastic decrease in the observed enthalpy values. Furthermore, within this concentration range, the peaks measured in the titration experiment change from indicating one fast endothermic process to a composite process with one fast endothermic process occurring together with a slower exothermic one, as can be seen in Figure 6.

The design of the calorimeter employed for these measurements and its principle of operation (based on power compensation) are such that its response to instantaneous processes would be over in a few minutes. This is the common response for similar experiments with dilution of surfactant solutions, and can be observed for the initial and final peaks for a typical titration experiment, shown in Figure 6. When the $C_{12}EO_6$ concentration in the calorimeter cell approached a molar ratio of 2, not only was a decrease in the overall heat exchanged

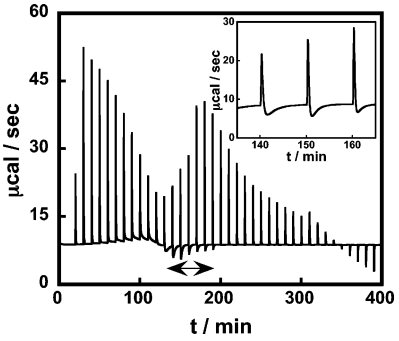

Figure 6. ITC raw data for addition of 10 wt % $C_{12}EO_6$ to 1.5 wt % P123 solution at 40 °C. Injections 12−18 (between arrows) give a composite peak with one fast endothermic process and a slower exothermic one; see inset. (The time between each injection in this experiment, 10 min, was too short to reach equilibrium. That took 15−20 min.)

observed, but also the peaks showed the appearance of a much slower exothermic process, which lasted up to 15−20 min (see the inset in Figure 6). Interestingly, a similar time dependence in the same concentration range was observed during the light scattering measurements (see below). For reasons stated above, this slower process differs from the dilution/interaction processes observed for smaller or larger molar ratios, and should be ascribed to another process, which occurs only in this concentration range.

Addition of $C_{12}EO_6$ to 0.05% F127 ($EO_{97}PO_{69}EO_{97}$) at 35 °C[31] and to 2.5% L64 ($EO_{13}PO_{30}EO_{13}$)[32] solutions at 40 °C gave positive enthalpy changes, which shows that $C_{12}EO_6$ interacts with copolymer aggregates from the lowest concentration (about 2×10^{-5} mol L^{-1}), in agreement with our observation. However, the enthalpy values determined in the beginning of these titration experiments are well above 30 kJ mol^{-1} and much larger than the ones we observed. The enthalpy changes then decrease to zero, joining the curve for dilution of $C_{12}EO_6$ in water where the titrations ended. No exothermic break was observed in those studies. A possible reason for the large initial enthalpy values is that a significant fraction of the F127 and L64 polymers were in the form of monomers. Added $C_{12}EO_6$ would induce further polymer aggregation, giving a large enthalpy contribution, in addition to the enthalpy change from $C_{12}EO_6$ being solubilized in the aggregates. DSC curves for F127 solutions shown in Figure 1b of ref 45 show that conversion to micelles is not complete in 0.05% at 35 °C. The same could be proposed to occur in L64 solutions at 40 °C.

Dynamic and Static Light Scattering. *Sphere-to-Rod Transition of P123−$C_{12}EO_6$ Aggregates.* DLS experiments were performed on P123−$C_{12}EO_6$ solutions of molar ratios varying from 0 to 11, in order to evaluate the apparent hydrodynamic radius of the mixed P123−$C_{12}EO_6$ aggregates (or micelles) below (spheres) and at (rods) the shape transition temperature. The transition temperature for each molar ratio was chosen as the maximum of the second peak T_m(sphere−rod) in the DSC experiments (Figure 2 and Table 1). All of the solutions contained 1.00 wt % with respect to P123. Figure 7 presents the normalized time pseudo-cross-correlation functions of the scattering intensity, $g^{(2)}(t) - 1$, for $C_{12}EO_6$/P123 molar ratios of MR = 2.2, 3.2, and 6.0 at two different temperatures.

The lower temperature was set at least 5 °C below the sphere-to-rod transition temperature, whereas the higher corresponds to the transition temperature for each molar ratio. The correlation function is shifted toward longer times at the higher temperature for all three solutions, and the difference between the two functions decreases with increasing molar ratio.

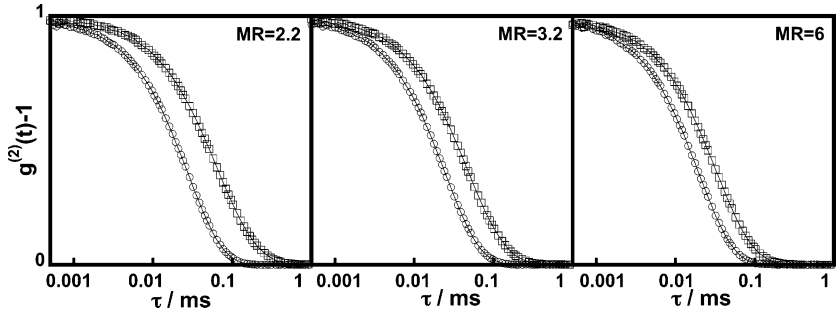

Figure 7. Correlation functions of the scattered light at $\theta = 90°$ at temperatures below (○) and at the sphere-to-rod transition (□) for mixed solutions containing 1.0 wt % P123 and with $C_{12}EO_6$/P123 molar ratios (MR) of 2.2, 3.2, and 6.

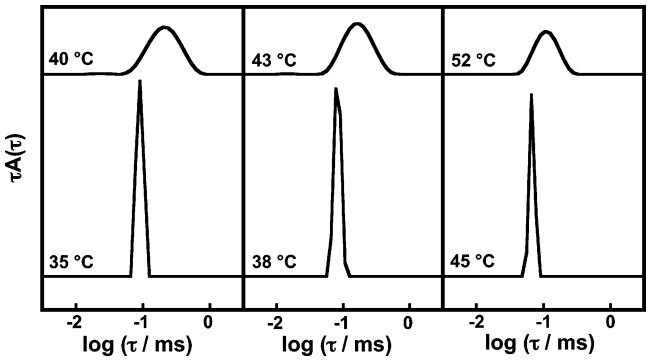

Figure 8. Relaxation time distributions obtained from inverse Laplace transformation of the intensity correlation functions shown in Figure 7 for $C_{12}EO_6$/P123 molar ratios of 2.2, 3.2, and 6 (from left to right). Distributions at the sphere-to-rod transition temperature (top) and below (bottom) are presented.

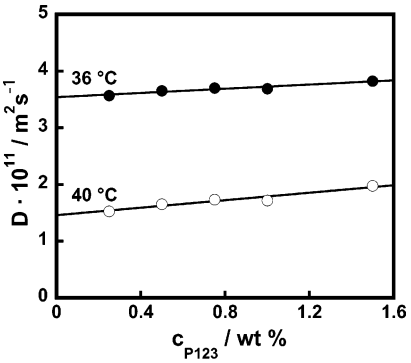

Figure 9. Diffusion coefficients as a function of copolymer concentration for mixed P123−$C_{12}EO_6$ micelles at a molar ratio of 2.2 at 36 °C (●, spherical shape) and at 40 °C (○, rodlike shape). The solid lines represent linear least-squares fits.

The corresponding relaxation time distributions obtained by inverse Laplace transformation of the $g^{(2)}(t) - 1$ functions are shown in Figure 8. The narrow distributions at the bottom of the figure correspond to systems of monodisperse spherical aggregates. The upper broader relaxation curves represent the relaxation time distributions of the system at equilibrium at the sphere-to-rod transition temperature. The broadening and the shift of the relaxation modes at the shape transition temperature indicate a growth of the P123−$C_{12}EO_6$ aggregates into larger and more polydisperse particles. The single relaxation modes seen in the distributions are diffusive. This was established from the linear q^2 dependences of the relaxation frequencies, Γ (see eq 3), obtained by performing DLS measurements at eight different scattering angles between 35 and 145° on each of the mixed solutions (data not shown).

For the lower molar ratios, the scattering intensity measured at a fixed angle and as a function of temperature presented a pronounced increase at a defined temperature, which corresponded well with the sphere-to-rod transition temperature obtained from the DSC results in Figure 2. For the solution with a molar ratio of 11, the scattering intensity showed a less distinct increase with increasing temperature than at lower molar ratios. At high molar ratios, for example, at MR = 46, the mixed micelles grow both with concentration and temperature and the behavior is more like the wormlike micelles of pure $C_{12}EO_6$.[34] Therefore, they do not show a distinct shape transition temperature.

The concentration dependence of the apparent mutual diffusion coefficients, D, of the spherical and the rodlike mixed aggregates was also analyzed. Solutions containing between 0.3 and 1.5 wt % of P123 and of $C_{12}EO_6$ to give a molar ratio of 2.2 were prepared, and D was determined from dynamic light scattering experiments at 36 and 40 °C. For each concentration, the apparent diffusion coefficients were evaluated from the slope according to eq 3. The results are summarized in Figure 9.

The positive slopes observed in the figure indicate a repulsive interaction between the P123−$C_{12}EO_6$ aggregates in solution. The hydrodynamic radii were derived using the Stokes−Einstein relation from the values of D extrapolated to zero copolymer concentration, D_0. At 36 °C, the mixed micelles are spheres with $R_H = 9.1 \pm 0.1$ nm. At 40 °C, R_H had increased to 24.1 $\pm$ 0.8 nm and the shape of the aggregates had become elongated. The hydrodynamic length, L, of the rodlike mixed micelles at MR = 2.2 was also estimated from D_0. In the model formulated by Tirado and Garcia de la Torre, the relation between D_0 and L is given by, see, e.g., ref 46:

$$D_0 = \frac{kT}{3\pi\eta_0 L}(\ln(L/d) + \nu) \qquad (5)$$

where d is the diameter of the rod and $\nu = 0.312 + [0.565/(L/d)] - [0.1/(L/d)^2]$ in the regime where $5 < L/d < 30$.

Assuming a rodlike particle with a cross-sectional radius equal to the radius of the sphere ($=R_H$ at infinite dilution) and using eq 5, a rod length of 104 nm was derived for the mixed micelle at molar ratio 2.2.

Static light scattering measurements were performed on the aqueous solution with a $C_{12}EO_6$/P123 molar ratio of 2.2 (and 1.00 wt % P123) at 40 °C to determine the apparent radius of gyration, $R_{g,app}$, of the rodlike mixed micelles using classical SLS analysis.[47] A value of $R_{g,app} = 46$ nm was found from the angular dependence of the scattered light (data not shown). The ratio of the radius of gyration to the hydrodynamic radius (R_g/R_H) also provides information about the internal morphology of the scattering particle.[48] For a perfect homogeneous sphere, $R_g/R_H \leq 0.775$, and for an infinite rod, it is >2.[49] The apparent

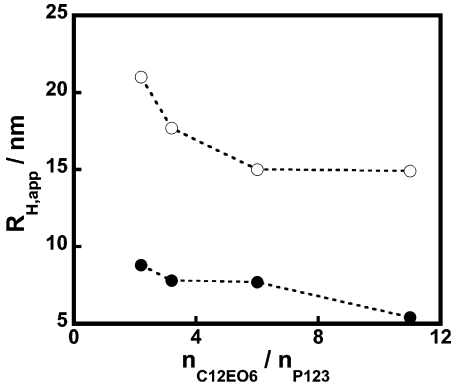

Figure 10. Apparent hydrodynamic radii for the mixed micelles as a function of molar ratio ($n_{C_{12}EO_6}/n_{P123}$). Values obtained from DLS measurements performed below the transition temperatures (●, spherical shape) and at the sphere-to-rod transition temperatures (○, rodlike shape). The following temperatures were used: 35 and 40 °C for MR = 2.2, 38 and 43 °C for MR = 3.2, 45 and 52 °C for MR = 6, and 25 and 60 °C for MR = 11.

values obtained in our SLS and DLS experiments, $R_{g,app} = 46$ nm and $R_{H,app} = 21$ nm, give a value larger than 2, which confirms the rodlike shape of the mixed micelle at MR = 2.2 and 40 °C. A rheological study performed in parallel on the same system (both at equilibrium and time-resolved measurements) presents clear evidence from the observation of shear-thinning effects that rodlike objects are formed at the transition temperature for this molar ratio.[50]

We were also interested in comparing the size of the aggregates at different molar ratios before and after the shape transition to correlate their size with the transition temperature. Values of $R_{H,app}$ of the mixed aggregates in 1.00 wt % P123 solutions with $C_{12}EO_6$/P123 molar ratios equal to 2.2, 3.2, and 6.0 are shown in Figure 10 at temperatures below and at the shape transition temperature in each case.

The data in Figure 10 reveal that the size of the mixed spherical micelles at temperatures below the transition temperature decreases with increasing $C_{12}EO_6$ content. This was established in a previous light scattering investigation, where the values of R_H of the spherical mixed micelles were analyzed at infinite dilution.[34] For example, at 40 °C, these DLS measurements gave $R_H = 10.1$, 9.9, 7.9, and 6.4 nm for mixed micelles with MR = 0, 0.6, 5.7, and 12, respectively. Figure 10 also shows that the size of rodlike aggregates at the shape transition temperature also decreases in terms of $R_{H,app}$ with increasing content of $C_{12}EO_6$.

Time-Resolved DLS and SLS. Time-resolved dynamic light scattering measurements were carried out on the $C_{12}EO_6$/P123 solution with a molar ratio of 2.2 (containing 1.00 wt % P123) when changing the temperature of the light scattering cell from 36 to 40 °C. Simultaneously, the static light scattering intensity at $\theta = 90°$ was monitored over short time intervals. The results are summarized in Figure 11 where the scattered intensity, I (normalized to the incoming laser intensity), as well as the temperature are plotted as functions of time.

After about 200 s when the temperature reached 39.5 °C, the intensity started to increase and the change became faster as the temperature approached 40 °C. After about 1800 s, the intensity started to level off but only slowly, and not until after about 3600 s did it become constant. The increase in intensity is due to an increase in size of the mixed P123−$C_{12}EO_6$ micelles, since larger particles scatter more (for impermeable spheres with radius R, I is proportional to R^6). The time-resolved experiments also showed that the sphere-to-rod transition is

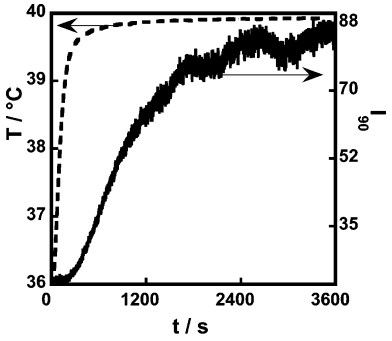

Figure 11. Static light scattering intensity normalized to the laser intensity (solid line) and temperature (dashed line) as functions of time for the mixed solution with a $C_{12}EO_6$/P123 molar ratio of 2.2 and 1.0 wt % with respect to P123. Measurements preformed at $\theta = 90°$.

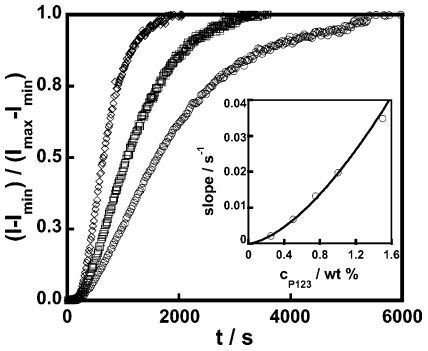

Figure 12. Normalized scattered intensity from SLS as a function of time for the mixed solution with a $C_{12}EO_6$/P123 molar ratio of 2.2 and with various amounts of P123: 0.50 wt % (○); 0.75 wt % (□); 1.5 wt % (◇). The inset presents the initial slope of the linear part of the intensity vs time for the MR = 2.2 solution as a function of the P123 concentration (0.25, 0.50, 0.75, 1.0, and 1.5 wt %).

reversible. DLS and SLS measurements at 25 °C gave the same values for the scattering intensity and apparent hydrodynamic radii before and after the temperature of the sample had been raised to 40 °C. The same time dependence of the light scattering intensity was also observed when two thermostatted stock solutions of P123 and $C_{12}EO_6$ were directly mixed to obtain a molar ratio of 2.2 in the light scattering cell at 40 °C after which the intensity recording started. The first technique with temperature increase was preferred, since it was easier to control the exact amount of each component in the mixed solution.

The growth process observed in Figure 11 is surprisingly slow. As indicated by the calorimetric titration curves, it is a complicated process that involves both diffusion and collision where material is rearranged to create larger elongated objects. The effect of total concentration on the rate of growth was investigated by varying the P123 concentration between 0.25 and 1.5 wt % but keeping the $C_{12}EO_6$/P123 molar ratio constant and equal to 2.2. Figure 12 shows the normalized scattered intensity expressed as $(I - I_{min})/(I_{max} - I_{min})$ against time for mixed solutions containing 0.5, 0.75, and 1.5 wt % with respect to P123 (the temperature scan is not shown); cf. Figure 11. The figure reveals the strong concentration dependence. An increase of the total concentration increases the rate of the process. It was a matter of hours to reach equilibrium in the 0.25 wt % solution, while in the 1.5 wt % solution it took about 1000 s (or 16 min) to reach the equilibrated state. In order for the mixed P123−$C_{12}EO_6$ micelles to change shape and grow from spheres to elongated rods, enough material is needed and that can only be achieved by an encounter with neighboring aggregates. The slope of the initial, linear part of the intensity curves may represent the rate of the growth process. The inset in Figure 12

shows a plot of the initial slopes (in s^{-1}) against copolymer concentration (at MR = 2.2). A power law function describes the data points. The rheological investigation of the same system did not show any slow kinetic effects at P123 concentrations above 5 wt %. However, for 1.5 wt % and MR = 2.2, the rheological technique was able to detect the slow growth of the mixed aggregates.[50]

Discussion

The phase behavior of PEO−PPO−PEO copolymers in water has been both investigated experimentally and modeled theoretically.[51−55] A general phenomenon in PEO-containing polymer (or surfactant) aqueous systems is the occurrence of a lower critical solution temperature (LCST), above which there is liquid−liquid phase separation.[56] It appears because the effective solute−solute interactions become more attractive at higher temperatures. One explanation for this behavior is that the −O−C−C−O− sequence in PEO changes into a less polar form as the temperature increases and therefore PEO interacts less favorably with water.[57] A weakened PEO−water interaction at elevated temperatures favors a higher packing density at the PPO−PEO interface, which in turn favors a change in the shape of the micelles from spherical to rodlike (or cylindrical). For the same reason, PEO−PPO−PEO−water systems often present a normal hexagonal liquid crystalline phase of cylindrical micelles at temperatures above that of the cubic phase, which consists of spherical micelles; see, e.g., refs 52 and 58.

In the present study, we have investigated the mixed system of the nonionic PEO−PPO−PEO copolymer $EO_{20}PO_{68}EO_{20}$ (P123) and the nonionic surfactant $C_{12}EO_6$. Even small additions of $C_{12}EO_6$ have surprisingly large effects on the liquid−liquid phase separation temperature (Figure 3). A minimum is observed at molar ratios between 2 and 3. The pure P123 micelles undergo a shape transition from spherical to rodlike at around 60 °C; see Table 1 and Figure 2. The mixed micelles formed upon addition of $C_{12}EO_6$ also show this change of shape at temperatures that vary with composition. The phase separation temperature and the sphere-to-rod transition temperature follow the same trend, presenting minima at molar ratios between 2 and 3 (Figures 2 and 3).

For the pure P123 micelle at 40 °C, the aggregation number is 131, as determined by using SLS, and for MR = 0.7, it is 127.[34] We propose that, for low molar ratios up to 2.2, the large PPO core of the spherical aggregate is not significantly affected by the solubilization of the $C_{12}EO_6$ surfactant molecules that will be located at the PPO−PEO interface. The fact that the apparent R_H values of the mixed spherical micelles are almost unchanged up to molar ratios of 2.2 compared to the pure P123 micelles (see Figure 10) supports this assumption. This means that the incorporation of the C_{12} alkyl chains does not affect the interior of the core and no unfavorable stretching of the PPO chains will occur. The relaxation of the PPO stretching when the PEO−PPO−PEO micelle changes from spherical to rodlike is one of the factors that drives the sphere-to-rod transition in the pure PEO−PPO−PEO systems.[21] The other one is the conformation change of the PEO groups. Therefore, we may focus the discussion on the PEO conformation at the core−corona (or PPO−PEO) interface of the micelles to explain their preferred shape. At the core−corona interface of the pure block copolymer micelles, the area per EO_{20} chain is such that the spherical form of the micelles is favored at ambient temperatures. This means that the area per PEO chain is large and the PEO conformation is therefore not completely stretched. It is expected that, at small additions of $C_{12}EO_6$ to the pure P123 micelles, the insertion of the surfactant molecules would lead to a separation of the EO_{20} chains at the core−corona interface, causing an increase in the area per EO_{20} group. Thus, the $C_{12}EO_6$ molecules would act as spacers. Zheng and Davis[59] have discussed this spacer effect in the mixed EO_{21}−EE_{35}−EO_{21} block copolymer−$C_{12}EO_5$ surfactant aqueous system, where EE denotes ethylethylene. In their system, the pure block copolymer micelles are cylindrical. This structure has a low curvature with stretched PEO corona chains. The addition of $C_{12}EO_5$ to the EO_{21}−EE_{35}−EO_{21} micelles allows the EO_{21} chains to relax and adopt a more coiled conformation, as the distance between the EO_{21} groups increases due to the insertion of the $C_{12}EO_5$ molecules at the core−corona interface. This gives a more curved interface, and the mixed micelles become spherical. However, in the P123−$C_{12}EO_6$ system, we do not observe the same effect, as the curvature of the pure P123 micelles is already large. We cannot tell whether the $C_{12}EO_6$ molecules act as spacers at low additions, since the spherical shape is the geometrical form that has the largest curvature of all possible geometries. As the addition of $C_{12}EO_6$ continues, still at molar ratios below 2 where the PPO core radius is unaffected, the effect is instead the opposite: the presence of the $C_{12}EO_6$ molecules with their shorter EO_6 chains at the PPO−PEO interface causes a decrease in the overall average PEO area. This decrease will facilitate a temperature-induced change from a spherical to a rodlike shape, and therefore, the sphere-to-rod transition temperature is lowered. In the region of molar ratios 2−3, both the shape transition and the phase separation temperatures are at the minimum; see Table 1 and Figures 2 and 3. At higher $C_{12}EO_6$ content, both transition temperatures increase. At a molar ratio of 6, the aggregation number of P123 has decreased to 52 (at 40 °C).[34] The core now consists of about 50 PPO blocks and 330 C_{12} chains, and we expect the core radius to be slightly smaller than that at lower molar ratios. The observed change in R_H from 10 to 8 nm (at 40 °C) supports this assumption.[34] This means that the curvature of the mixed micelles at a molar ratio of 6 is larger than at a molar ratio of 2. In order to change the curvature into a state that fits a rodlike shape, more energy needs to be put into the system. A larger curvature of the smaller micelles explains why the sphere-to-rod transition temperature for MR = 6 is higher than that at MR = 2 (Table 1).

The PEO−PPO−PEO copolymers are polydisperse both in mass and composition. This causes the micellization process to occur in a concentration range or a temperature range rather than at a specific critical concentration or temperature.[9,19,60,61] This is manifested in a broad unimer-to-micelle temperature region, which is seen as a broadening of the main transition peak in the DSC experiments (Figure 1a). For the mixed P123−$C_{12}EO_6$ system, a shoulder appeared on the low-temperature side of the DSC peak at molar ratios of 0.7 and 1.1 and the main peak became broader (Figure 1a). This shoulder was only seen for low additions of $C_{12}EO_6$. At a molar ratio of 2.2, the peak has moved to the position of the shoulder and also become narrower. The mixed system consists at low temperature of P123 unimers and $C_{12}EO_6$ micelles. When the temperature increases, aggregates start to form at a considerably lower temperature than in pure P123 solution. The shoulder in the DSC peaks could indicate that a new species was formed, i.e., mixed micelles with a defined stoichiometry. At a molar ratio of 2.2, the shoulder was replaced by a well-defined peak, indicating complete conversion to micelles of about this composition. As we have not investigated the variation of the DSC peaks with composition in any more detail, we assume for the sake of

simplicity that the mixed micelles contain two $C_{12}EO_6$ molecules per P123 molecule. The enthalpy of aggregation, ΔH_{agg}, of the mixed micelle, calculated per mole of P123, is not significantly changed, but the temperature, T_m, has decreased 5 °C compared to that of pure P123; see Table 1. The formation of mixed micelles with a 2:1 composition is compatible with the pronounced minima in the sphere-to-rod and liquid−liquid phase separation temperatures at $C_{12}EO_6$/P123 molar ratios in the range 2−3.

The titration of $C_{12}EO_6$ into P123 solution at 40 °C gave endothermic interaction enthalpies followed by a sharp exothermic minimum at a molar ratio between 2 and 3 depending on the P123 concentration (Figure 5). After the minimum, the interaction enthalpies were again endothermic but smaller than before. An inspection of the DSC curves in Figure 2 gives a possible reason for this exothermic peak. On the basis of results from the light scattering experiments, we ascribe the small broad peak in the DSC curves to a sphere-to-rod transition of mixed micellar aggregates. According to the curves, the onset temperature of this peak decreases with increasing $C_{12}EO_6$ content from 51 °C at a molar ratio of MR = 1.1 to 38 °C at MR = 2.2 and then increases to 41 °C at MR = 3.2 and further to 48 °C at MR = 6. This implies that at MR = 2.2 all mixed aggregates are in the form of spheres at temperatures below 38 °C and in the form of rods above 46 °C. The sphere-to-rod transition is endothermic by about 10 kJ mol^{-1}. The isothermal calorimetric experiments at 40 °C cross the lower part of the DSC peak for MR = 2.2. If we use Figure 2 to envisage what happens during the titration when adding $C_{12}EO_6$ to a P123 solution at 40 °C (Figure 5), we can see that, in the beginning at low molar ratios, the mixed micelles are spherical and continue to be so until we reach a MR of about 2 where rods will start to form. Increasing the $C_{12}EO_6$ content further, more rods are formed, but then, at a MR above 3, all of the aggregates become spheres again. Thus, the rods exist over only a narrow concentration range. The formation of spheres from rods will be exothermic, which gives the sharp exothermic peak in the calorimetric titration curves (Figure 5). The endothermic change we could expect to see when the rods form from spheres is probably hidden in the endothermic enthalpy changes we measure before the exothermic peak.

Acknowledgment. We wish to acknowledge the financial support of the Swedish Research Council (VR) and the Linneus Center of Excellence "Organizing Molecular Matter" (K.S.), the Swedish Foundation for Strategic Research (SSF) (D.L.), and the Brazilian Agencies FAPESP and CNPq (W.L., A.N.).

References and Notes

(1) *Nonionic Surfactants: Polyoxyalkylene Block Copolymers*; Nace, V. M., Ed.; Marcel Dekker, Inc.: New York, 1996; Vol. 60.

(2) Brochure *Pluronic and Tetronic Surfactants*; BASF Performance Chemicals, BASF Corp.: Mount Olive, NJ, 1996.

(3) *Amphiphilic Block Copolymers: Self-Assembly and Applications*; Alexandridis, P., Lindman, B., Eds.; Elsevier Science, BV: Amsterdam, The Netherlands, 2000.

(4) Wu, J.; Xu, Y.; Dabros, T.; Hamza, H. *Colloids Surf., A* **2005**, *252*, 79.

(5) Fusco, S.; Borzacchiello, A.; Netti, P. A. *J. Bioact. Compat. Polym.* **2006**, *21*, 149.

(6) Kabanov, A. V.; Alakhov, V. Y. *Crit. Rev. Ther. Drug Carrier Syst.* **2002**, *19*, 1.

(7) Al-Saden, A. A.; Whately, T. L.; Florence, A. T. *J. Colloid Interface Sci.* **1982**, *90*, 303.

(8) Rassing, J.; Attwood, D. *Int. J. Pharm.* **1983**, *13*, 47.

(9) Brown, W.; Schillén, K.; Almgren, M.; Hvidt, S.; Bahadur, P. *J. Phys. Chem.* **1991**, *95*, 1851.

(10) Mortensen, K.; Brown, W. *Macromolecules* **1993**, *26*, 4128.

(11) Pedersen, J. S.; Gerstenberg, M. C. *Colloids Surf., A* **2003**, *213*, 175.

(12) Beezer, A. E.; Loh, W.; Mitchell, J. C.; Royall, P. G.; Smith, D. O.; Tute, M. S.; Armstrong, J. K.; Chowdhry, B. Z.; Leharne, S. A.; Eagland, D.; Crowther, N. J. *Langmuir* **1994**, *10*, 4001.

(13) Alexandridis, P.; Holzwarth, J. F.; Hatton, T. A. *Macromolecules* **1994**, *27*, 2414.

(14) Alexandridis, P.; Hatton, T. A. *Colloids Surf., A* **1995**, *96*, 1.

(15) Mortensen, K. *J. Phys.: Condens. Matter* **1996**, *8*, A103.

(16) Chu, B.; Zhou, Z. In *Nonionic Surfactants: Polyoxyalkylene Block Copolymers*; Nace, V. M., Ed.; Marcel Dekker, Inc.: New York, 1996; Vol. 60; p 67.

(17) Mortensen, K.; Pedersen, J. S. *Macromolecules* **1993**, *26*, 805.

(18) Schillén, K.; Brown, W.; Johnsen, R. M. *Macromolecules* **1994**, *27*, 4825.

(19) Batsberg, W.; Ndoni, S.; Trandum, C.; Hvidt, S. *Macromolecules* **2004**, *37*, 2965.

(20) Michels, B.; Waton, G.; Zana, R. *Colloids Surf., A* **2001**, *183−185*, 55.

(21) Linse, P. *J. Phys. Chem.* **1993**, *97*, 13896.

(22) Jørgensen, E. B.; Hvidt, S.; Brown, W.; Schillén, K. *Macromolecules* **1997**, *30*, 2355.

(23) Wu, Y. L.; Sprik, R.; Poon, W. C.; Eiser, E. *J. Phys.: Condens. Matter* **2006**, *18*, 4461.

(24) Aswal, V. K.; Kohlbrecher, J. *Chem. Phys. Lett.* **2006**, *425*, 118.

(25) Nagarajan, R.; Barry, M.; Ruckenstein, E. *Langmuir* **1986**, *2*, 210.

(26) Nagarajan, R.; Ganesh, K. *J. Colloid Interface Sci.* **1996**, *184*, 489−499.

(27) Gadelle, F.; Koros, W. J.; Schechter, R. S. *Macromolecules* **1995**, *28*, 4883.

(28) Caragheorgheopol, A.; Caldararu, H.; Dragutan, I.; Joela, H.; Brown, W. *Langmuir* **1997**, *13*, 6912.

(29) Causse, J.; Lagerge, S.; de Ménorval, L.-C.; Faure, S.; Fournel, B. *Colloids Surf., A* **2005**, *252*, 51.

(30) Lettow, J. S.; Lanchaster, T. M.; Glinka, C. J.; Ying, J. Y. *Langmuir* **2005**, *21*, 5738.

(31) Couderc, S.; Li, Y.; Bloor, D. M.; Holzwarth, J. F.; Wyn-Jones, E. *Langmuir* **2001**, *17*, 4818.

(32) Couderc-Azouani, S.; Sidhu, J.; Thurn, T.; Xu, R.; Bloor, D. M.; Penfold, J.; Holzwarth, J. F.; Wyn-Jones, E. *Langmuir* **2005**, *21*, 10197.

(33) Hossain, K. M.; Hinata, S.; Lopez-Quintela, A.; Kunieda, H. *J. Dispersion Sci. Technol.* **2003**, *24*, 411.

(34) Schillén, K.; Jansson, J.; Löf, D.; Costa, T. Manuscript in preparation.

(35) Glatter, O.; Fritz, G.; Lindner, H.; Brunner-Popela, J.; Mittelbach, R.; Strey, R.; Egelhaaf, S. U. *Langmuir* **2000**, *16*, 8692.

(36) Schurtenberger, P.; Cavaco, C.; Tiberg, F.; Regev, O. *Langmuir* **1996**, *12*, 2894.

(37) Jansson, J.; Schillén, K.; Olofsson, G.; da Silva, R. C.; Loh, W. *J. Phys. Chem. B* **2004**, *108*, 82.

(38) Stepanek, S. In *Dynamic Light Scattering: The Method and Some Applications*; Brown, W., Ed.; Oxford University Press: Oxford, U.K., 1993; p 177.

(39) Vink, H. *J. Chem. Soc., Faraday Trans. 1* **1985**, *81*, 1725.

(40) Grell, E.; Lewitzki, E.; Schneider, R.; Ilgenfritz, G.; Grillo, I.; von Raumer, M. *J. Therm. Anal.* **2002**, *68*, 469.

(41) Ilgenfritz, G.; Schneider, R.; Grell, E.; Lewitzki, E.; Ruf, H. *Langmuir* **2004**, *20*, 1620.

(42) Olofsson, G. *J. Phys. Chem.* **1985**, *89*, 1473.

(43) Kaneshina, S.; Shibata, O.; Nakamura, M. *Bull. Chem. Soc. Jpn.* **1982**, *55*, 951.

(44) Comment: Values for the enthalpy of micelle formation of $C_{12}EO_6$ in water at 15 and 20 °C that can be derived from titration curves shown in Figures 3 and 4 of ref 31 and at 25 °C from Figure 13 of ref 32 are 4.3−5.0 kJ/mol lower than results reported in ref 42. We have no explanation for this discrepancy.

(45) da Silva, R. C.; Olofsson, G.; Schillén, K.; Loh, W. *J. Phys. Chem. B* **2002**, *106*, 1239.

(46) Borsali, R.; Nguyen, H.; Pecora, R. *Macromolecules* **1998**, *31*, 1548.

(47) Kratochvil, P. *Classical Light Scattering from Polymer Solutions*; Elsevier Science Publishers B. V.: Amsterdam, The Netherlands, 1987.

(48) Burchard, W.; Schmidt, M.; Stockmayer, W. H. *Macromolecules* **1980**, *13*, 1265.

(49) Burchard, W. *Adv. Polym. Sci.* **1999**, *143*, 113.

(50) Löf, D.; Schillén, K.; Torres, M. F.; Müller, A. J. Manuscript in preparation.

(51) Wanka, G.; Hoffmann, H.; Ulbricht, W. *Macromolecules* **1994**, *27*, 4145.

(52) Zhang, K.; Khan, A. *Macromolecules* **1995**, *28*, 3807.

(53) Hecht, E.; Mortensen, K.; Hoffnann, H. *Macromolecules* **1995**, *28*, 5465.

(54) Alexandridis, P.; Olsson, U.; Lindman, B. *Langmuir* **1998**, *14*, 2627.

(55) Svensson, M.; Alexandridis, P.; Linse, P. *Macromolecules* **1999**, *32*, 637.
(56) Holmberg, K.; Jönsson, B.; Kronberg, B.; Lindman, B. *Surfactants and Polymers in Aqueous Solution*; John Wiley & Sons, Ltd.: Chichester, U.K., 2003.
(57) Karlström, G. *J. Chem. Phys.* **1985**, *89*, 4962.
(58) Glatter, O.; Scherf, G.; Schillén, K.; Brown, W. *Macromolecules* **1994**, *27*, 6046.
(59) Zheng, Y.; Davis, H. T. *Langmuir* **2000**, *16*, 6453.
(60) Linse, P. *Macromolecules* **1994**, *27*, 6404.
(61) Hvidt, S.; Trandum, C.; Batsberg, W. *J. Colloid Interface Sci.* **2002**, *250*, 243.